Current Problems in Diagnostic Radiology 48 (2019) 251–261

Current Problems in Diagnostic Radiology

journal homepage: www.cpdrjournal.com

Angiomyolipoma of the Kidneys: Current Perspectives and Challenges in Diagnostic Imaging and Image-Guided Therapy

Abdul Razik, MD, Chandan J. Das, MD, DNB*, Sanjay Sharma, MD, DNB, FRCR

Department of Radiology, All India Institute of Medical Sciences (A.I.I.M.S), New Delhi, India

Angiomyolipomas (AML) are benign tumors of the kidneys frequently encountered in radiologic practice in large tertiary centers. In comparison to renal cell carcinomas (RCC), AML are seldom treated unless they are large, undergo malignant transformation or develop complications like acute hemorrhage. The common garden triphasic (classic) AML is an easy diagnosis, however, some variants lack macroscopic fat in which case the radiologic differentiation from RCC becomes challenging. Several imaging features, both qualitative and quantitative, have been described in differentiating the 2 entities. Although minimal fat AML is not entirely a radiologic diagnosis, the suspicion raised on imaging necessitates sampling and potentially avoids an unwanted surgery. Recently a new variant, epitheloid AML has been described which often has atypical imaging features and is at a higher risk for malignant transformation. Apart from the diagnosis, the radiologist also needs to convey information regarding nephrometric scores which help in surgical decision-making. Recently, more and more AMLs are managed with selective arterial embolization and percutaneous ablation, both of which are associated with less morbidity when compared to surgery. The purpose of this article is to review the imaging and pathologic features of classic AML as well as the differentiation of minimal fat AML from RCC. In addition, an overview of nephrometric scoring and image-guided interventions is also provided.

Introduction

Angiomyolipomas (AML) are benign tumors of mesenchymal origin primarily seen in the kidneys and having an overall prevalence of 0.44%.[1] In a retrospective analysis of 916 patients who underwent partial nephrectomy for presumed renal cell carcinoma (RCC), angiomyolipoma was the second most common pathology (28.7%) after oncocytoma (51.2%).[2] Classic AMLs are easily diagnosed radiologically and do not require treatment unless they are symptomatic or large. A subset of AMLs are lipid-poor and the diagnosis may not be straight forward on imaging. Several imaging features have been assessed till date in differentiating lipid-poor AMLs from RCCs since they may have radically different management. Recently, a newer histologic variant, epitheloid AML, has been described which has atypical imaging findings and malignant potential. Surgery (partial nephrectomy) is the most commonly performed surgery in symptomatic AML and the radiologists can often guide the surgeon in assessing the ease of resection by providing nephrometric scores. Of late, selective arterial embolization (SAR) has superceded surgery as the treatment of choice. Newer, less invasive percutaneous ablation techniques are also gaining popularity with active research being undertaken. This article attempts to elaborate the imaging findings of classic AML as well as those features which can potentially differentiate lipid-poor AML from RCC. Nephrometric scoring is discussed along with a review of newer concepts in image-guided interventions.

Clinical Presentation

AMLs most commonly present in the fourth to sixth decades of life and have a 4:1 female predilection. Most (80%) are sporadic, whereas hereditary tumors occur in association with tuberous sclerosis complex (TSC) and sporadic lymphangioleiomyomatosis (LAM). Nearly 55%-75% of the patients with TSC and 50% of those with sporadic LAM develop AML during their lifetime.[3-5] Among AMLs, 20% are associated with TSC. Syndromic AMLs present earlier and tend to be multifocal and bilateral. Extrarenal involvement (liver, spleen, uterus, and fallopian tubes) may also be seen. Syndromic AMLs also have faster growth rate, attain larger mean size and posses higher rate of complications.[6]

AMLs present with nonspecific symptoms. Most smaller lesions are asymptomatic and detected during routine imaging or screening for TSC. Confluent lesions with significant parenchymal replacement may cause renal failure and secondary hypertension.[7,8] Larger lesions may present as palpable lumps. AMLs larger than 4 cm develop elastin-poor vascular structures as well as aneurysms, and has 50% tendency to bleed.[9] When such spontaneous renal or perirenal hemorrhage occurs, the patient presents

ORCID number: Abdul Razik (0000-0002-3459–9467), Chandan J. Das (0000-0001-6505-5940).

Author contributions: All authors equally contributed to this paper with the conception and design, literature review and analysis, drafting, critical revision and editing, and approval of the final version.

* Reprint requests: Chandan J. Das, Department of Radiology, All India Institute of Medical Sciences, Ansari Nagar, 110029 New Delhi, India.

E-mail address: dascj@yahoo.com (C.J. Das).

https://doi.org/10.1067/j.cpradiol.2018.03.006
0363-0188/

with acute flank pain, palpable tender lump, and gross hematuria (Lenk's triad). This condition, described as Wunderlich syndrome, requires urgent embolization or surgery.[10] Hemorrhage can also be triggered by minor trauma and pregnancy.[11] Subcapsular hemorrhage over time may cause compression of the kidney, resulting in chronic compressive ischemic nephropathy (Page kidney).[12]

Etiopathogenesis, Genetics, and Classification

Initially considered a hamartoma, the neoplastic nature of AML and the clonal origin of its components have just been elucidated.[13] The World Health Organization (WHO) classifies AMLs among perivascular epithelioid cell tumors (PEComas), which also includes lymphangioleiomyomas, clear cell "sugar" tumor of the lung and clear cell myomelanocytic tumors.[14] These tumors are characterized by the presence of perivascular epithelioid cells (PEC), which typically are radially arranged around vessels, have clear or granular cytoplasm and central nucleus with small nucleoli.[15] PEC do not have any normal tissue counterpart and express melanocytic (HMB-45 and melan-A) as well as myocytic markers (smooth muscle actin). The origin of these tumors is controversial and has been variably attributed to neural crest cells, smooth muscles and pericytes.[16]

Classic AML, the most common type, is characterized by varying amounts of epithelioid and spindle cells, abnormal thick walled blood vessels and fat (triphasic morphology). It has a benign course and complications arise only in large tumors. Nodal involvement in classic AML is rare, almost always occurs in the context of TSC, and has been suggested to be a consequence of multifocal disease rather than metastatic spread.[17,18] Vascular invasion also may be seen with classic AML and does not necessarily indicate malignancy.[19-21] Cystic AML consists of epithelial cysts lined by cuboidal cells positive for cytokeratin.[22]

Epithelioid AML (EAML) is a recently described aggressive variant characterized by sheets of epithelioid cells demonstrating melanocytic markers. The term EAML is used only when the proportion of epitheloid cells exceeds 10%.[23] Pure EAMLs are extremely rare and are strongly associated with TSC. Malignant transformation is seen in a third of EAMLs. Recurrence, metastatic lymph node involvement, intravascular extension and hematogeneous metastasis are common, necessitating close follow up. The pathologic features predictive of malignancy are presence of $>70\%$ atypical epitheloid cells, >2 mitosis per HPF, atypical mitotic figures and necrosis.[24] Acquisition of P53 mutation is thought to be the trigger for malignant transformation.[25] Many cases of renal cell carcinomas previously described in TSC could have originally been malignant epithelioid AMLs.[3,26]

TSC is an autosomal dominant disorder resulting from heterozygous mutations of TSC1 and TSC2 genes located on 9q and 16p chromosomes, respectively. These genes code for the tumor suppresser proteins hamartin and tuberin, which normally downregulate the mechanistic target of rapamycin (mTOR) signaling cascade. Mutations of TSC2, but not TSC1, have also been observed in sporadic AML and other PEComas.[27-29]

Radiologic Findings of Classic AML

Plain radiographs are insensitive to small renal masses, whereas large fat containing masses may show up as areas of relative lucency compared to the adjacent soft tissue. Mass effect on the colon and bowel may be apparent. Intravenous urogram may demonstrate distortion of the pelvicalyceal system or the ureters. Lymphangioleiomyomatosis of the renal pelvis is seen rarely along with AML in TSC and may cause plaque like projection within the renal pelvis.[30,31] In TSC or LAM, multiple small, round and uniformly sized pulmonary cysts sparing the costophrenic angles are often seen.

Multidetector computed tomography (CT) and magnetic resonance imaging (MRI) are extremely useful in diagnosing AML, assessing their size, extent and for evaluating complications. A routine CT protocol includes noncontrast images, corticomedullary (35-45 second) nephrographic (90-120 second), and excretory phase images (3-5 minutes). Noncontrast images can be avoided if dual-energy CT is available. MRI protocol should include fat suppressed T2-weighted images, nonfat suppressed dual-gradient echo (in-phase and opposed-phase) T1-weighted images, fat suppressed T1-weighted images, diffusion-weighted images as well as postcontrast images in the corticomedullary, nephrographic and excretory phases. On CT, most AMLs appear as small "ball type" renal cortical masses having variable proportion of fat (−10 to −120 Hounsfield units) and enhancing soft tissue (Fig 1A-C). These masses fit into a wedge shaped defect in the kidney and have an angular or pyramidal morphology at the interface with the apex pointed towards the renal parenchyma. The base of the lesion contacts the renal capsule and often bulges beyond the renal contour exophytically into the perirenal fat. This angular or pyramidal morphology at the interface, first described by Verma et al,[32] is seen in 76% of AMLs and has 100% positive predictive value in differentiating benign from malignant renal masses. This feature has been attributed to the soft and flexible consistency of AML unlike the more solid tumors like renal cell carcinoma (RCC).

The presence of fat in a renal mass offers a reasonably specific diagnosis AML.[33] Even small amounts of fat can be appreciated on thin slice MDCT, aided by its high spatial resolution and excellent fat to soft tissue contrast. However, the technique of assessment has to be meticulous to avoid false positive observations. Areas of fat attenuation may not be apparent due to partial volume effect if the regions of interest (ROI) are drawn on thick sections.[33] Sequential rather than helical scanning can result in small portions of fat being missed due to respiratory misregistration.[34] The margins of ROI have to be drawn atleast 3 mm from the perirenal or renal sinus fat to avoid volume averaging. Many different thresholds of attenuation have been used till date for the identification of small amounts fat. Most studies support a threshold of −10 HU as being reasonably sensitive and specific.[33,35,36] Davenport et al[36] suggested that an ROI of atleast 19-24 mm^2 be used to avoid sampling stochastic noise (quantum mottle) and erroneously diagnosing fat.

Pixel mapping may be done to look for smaller clusters of fat and is more sensitive than ROI attenuation measurement.[37,38] A line or square of four contiguous pixels of attenuation less than −10 HU is considered indicative of the presence of fat.[35] The effectiveness of CT histogram analysis (pixel distribution analysis) has been variably reported.[39-42] Kim et al observed sensitivity, specificity of 44% and 88% for histogram analysis when a cut off of 1% pixels with attenuation less than −10 HU was used to differentiate AML from RCC.[39] Takahashi observed pixel distribution analysis to be no better than subjective evaluation in identifying small clusters of fat, however, concluded that skewness lower than −0.4 in whole-lesion-ROI texture analysis could identify fat in the lesion.[43]

Radiologic Findings of Minimal Fat AML

Approximately, 4.5% of classic AMLs show no macroscopic fat even on thin slice noncontrast CT (Fig 1D). These have been labeled "fat poor" or "minimal fat" AML.[44,45] A histologic definition

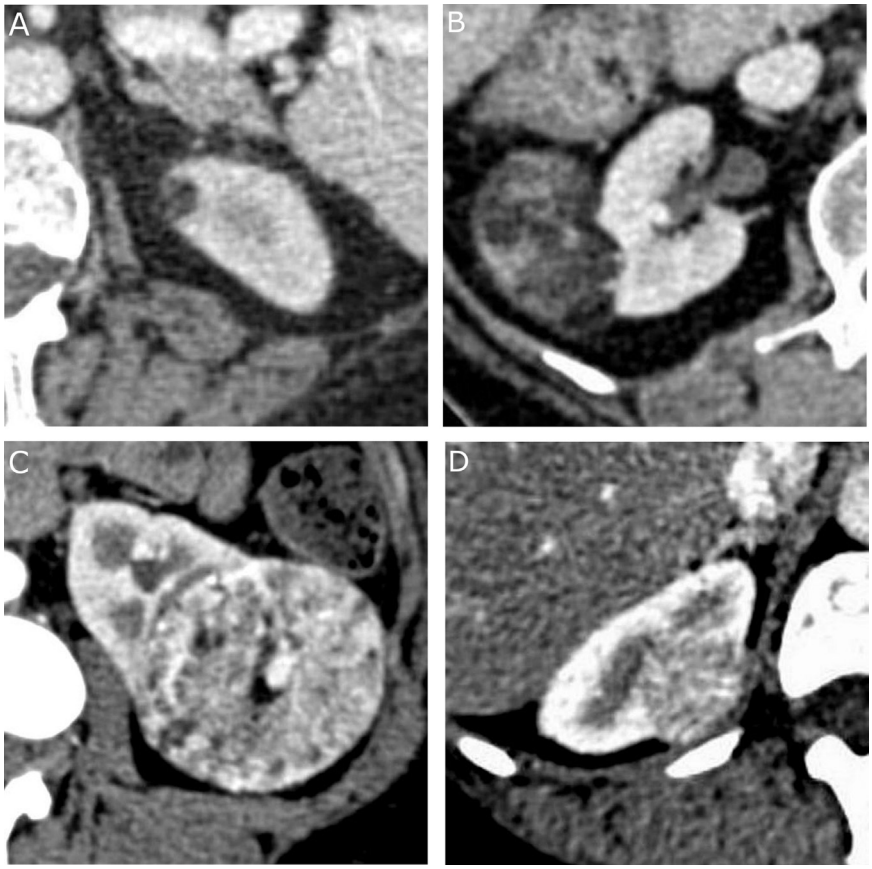

FIG 1. Spectrum of the morphology of renal angiomyolipomas (AML). Renal AMLs can exist as (A) small angular lesions fitting into wedge shaped cortical defects with their outer margins being flush with the renal capsule. (B) Further enlargement causes large exophytic component bulging into the perirenal space. (C) Variable amount of enhancing component may be present along with large intratumoral vessels. (D) Absence of macroscopic fat in AMLs (minimal fat AMLs) can create diagnostic dilemma; however, the angular morphology is still appreciable in most cases.

of less than 25% fat cells in per high power field has been used for minimal fat AML.[46] In some cases, the presence of significant acute hemorrhage may obscure the intralesional fat.

Several imaging features have been used to differentiate minimal fat AML from RCCs (Table 1 and Fig 2). This differentiation is relevant since most RCCs have poorer prognosis in comparison to AML, with some requiring radical surgery. Also the chemotherapy regimens used for RCC are different from those used for AML. Jinzaki et al[47] suggested that the absence of "beak" or "claw" sign in a lesion which protrudes from the renal margin indicates subcapsular or capsular origin and hence an AML.[48] Presence of "beak" sign would suggest tumors of parenchymal origin (including RCCs). Jinzaki also observed that AMLs tend to be homogeneously hyperattenuating on noncontrast scans, showed homogeneous enhancement on postcontrast phase. Clear cell RCCs, on the other hand show heterogeneous hyperenhancement, necrosis and hemorrhage.[38,47,49-51] Relative tumor attenuation can be quantified on noncontrast scans by using tumor-to-cortex ratio.[52] However, this finding lacks specificity as several other lesions (papillary RCC, renal metastasis from thyroid carcinoma, and benign complicated cysts and leiomyoma) may show similar appearance.[53,54] In addition, hemorrhage within the AML could result in heterogeneity.

Of late, attempts have been made to quantify tumor heterogeneity not visible to the human eye using software-aided texture analysis.[55,56] Hodgdon et al[56] observed that CT histogram analysis was useful in differentiating minimal fat AML from RCC on unenhanced scans. Among the texture parameters used, gray-level homogeneity and entropy were the strongest predictors. RCC showed significantly lesser homogeneity and higher entropy than minimal fat AML. The software-aided measurement of heterogeneity outperformed subjective assessment by radiologists. However, no attempt was made to apply these findings to each subtype of RCC. Recently a computer-aided classification system using texture parameters as well as histogram analysis has also been proposed to differentiate clear cell RCC and AML.[57]

TABLE 1
Differentiating features between minimal fat angiomyolipoma and renal cell carcinoma

Imaging features	Angiomyolipoma	Renal cell carcinoma
Angular morphology	+	–
Absence of beak sign	+	–
Density (NCCT)	Homogenous and hyperdense	Heterogenous*
T2 signal	Homogenous and hypointense	Heterogenous*
Necrosis and calcification	–	+
Hyperdense rim	+	–
Peritumoral vessels	–	+
Coexistent classic AML	+	–
Early enhancement	+	–**
Signal loss on OP images	+	–**
^{18}F-FDG PET uptake	–	+***
^{11}C-acetate PET uptake	+	–***

AML, angiomyolipoma; RCC, renal cell carcinoma; NCCT, noncontrast CT; FDG, fluorodeoxyglucose; PET, positron emission tomography.

* Except for papillary RCC.
** Except for clear cell RCC.
*** Except for chromophobe RCC.

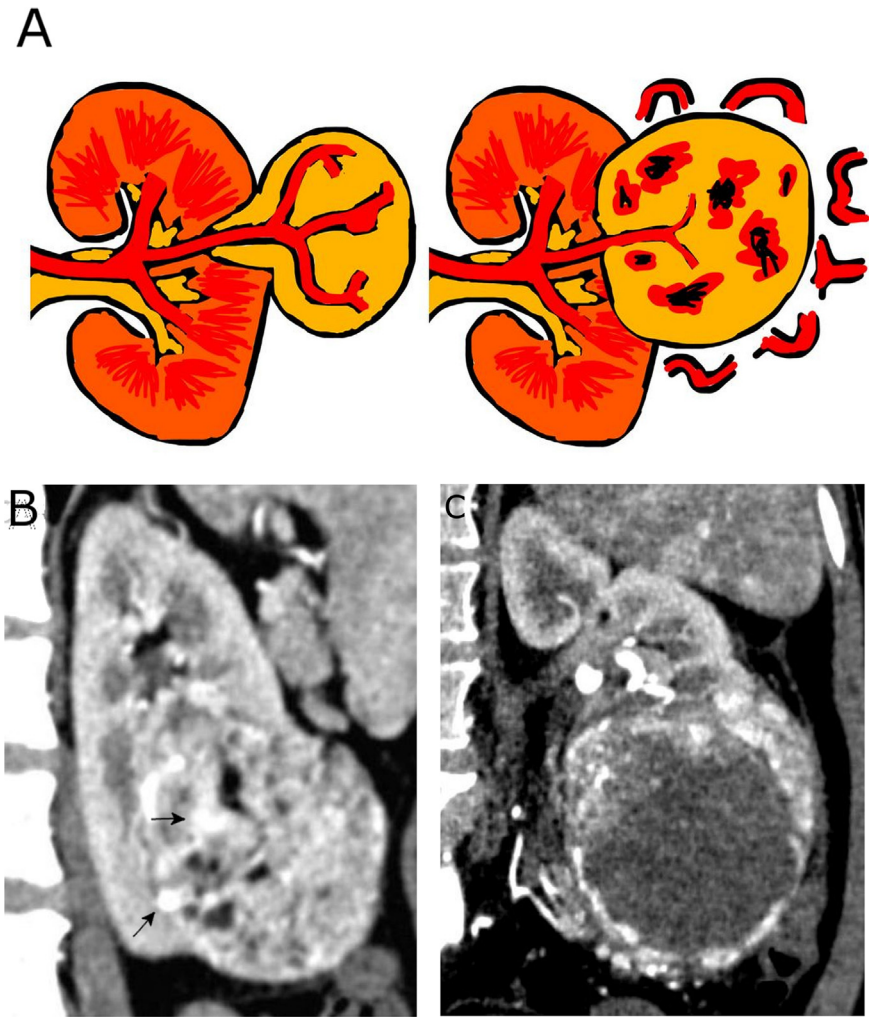

FIG 2. Differentiating features between AML and RCC. (A) AMLs (left) are characterized by angular morphology, large intratumoral vessels often with focal aneurysms, lack intralesional necrosis and hemorrhage. RCCs (right) demonstrate beak sign, lack angular morphology, possess intralesional hemorrhage and necrosis, and often have tortuous peritumoral collateral vessels. (B) A case of classic AML showing enhancing components and intralesional aneurysms (*arrows*). Note the clear perilesional fat. (C) A case of clear cell RCC showing large central area of necrosis and prominent peritumoral collateral vessels. (Color version of the figure available online.)

Angular interface, a morphologic feature described earlier has also been observed in minimal fat AMLs unlike RCCs.[49] As AML does not promote angiogenesis or inflammatory reaction, peritumoral collateral vessels are rarely seen in AMLs. Yang et al[49] observed that presence of peritumoral collateral vessels showed 100% negative predictive value for the diagnosis of AML.

Unlike RCC, calcification is extremely unusual in AMLs and its presence in an otherwise typical AML necessitates sampling to rule out RCC.[55,58] Yang et al also observed the presence of a hyperattenuating tumor rim to be a useful predictor of minimal fat AML; however, the same observation was not supported by other studies.[59] Presence of coexistent fat abundant AMLs also has been observed to be a suggestive sign of AML in TSC; however, fat containing RCC is also a remote possibility since patients with TSC have increased risk for RCCs as well.[3,49] Involvement of other organs may be seen in TSC (Fig 3). Numerous, large AMLs in TSC might cause complete renal parenchymal replacement.

On T2-weighted MRI, AMLs generally are uniformly hypointense (Fig 4A). Opposed and in-phase gradient-echo (GRE) MR images (chemical shift imaging) have been widely used to identify microscopic amounts (intravoxel or intracellular) of fat. Minimal fat AML shows significant drop in signal intensity (SI) on opposed-phase images (Fig 4B and C).[59,60] Kim et al[60] noted sensitivity and specificity of 96% and 93%, respectively for GRE when SI index of 25% and tumor-to-spleen ratio of −32% were used as cut-off. However, this rule cannot be generalized since clear cell RCC also is known to contain microscopic, intravoxel fat.[51,52] One study observed that presence of qualitative (visually detectable) signal loss on opposed-phase images was more suggestive of clear cell RCC than AML with a percentage SI drop of 29% being 100% specific for the former.[61] This author used tumor-to-kidney percentage signal drop rather than SI index (which lacks an internal reference) and tumor-to-spleen ratio (which is unreliable in patients with iron overload). Hindman et al observed that the presence of intravoxel fat in any small mass (< 2 cm) which is homogeneously hypointense on T2-weighted images suggests AML over clear cell RCC. Presence of necrosis is highly predictive of clear cell RCC.[62] However, if microscopic fat is not evident on GRE, hypointense signal on T2-weighted images can be seen with papillary RCCs and lymphomas as well. Diffusion restriction may be present within the enhancing components of the tumor (Fig 4D and E).

Dynamic enhancement is not useful in differentiating minimal fat AML from RCCs as a whole group since each variant of RCC shows a different enhancement pattern.[49] Clear RCCs show early intense enhancement and delayed washout. Oncocytomas show intense enhancement which peaks in the nephrographic phase, followed by rapid washout. AMLs and papillary RCCs show less intense wash-in and prolonged retention of contrast.[4,58,63,64]

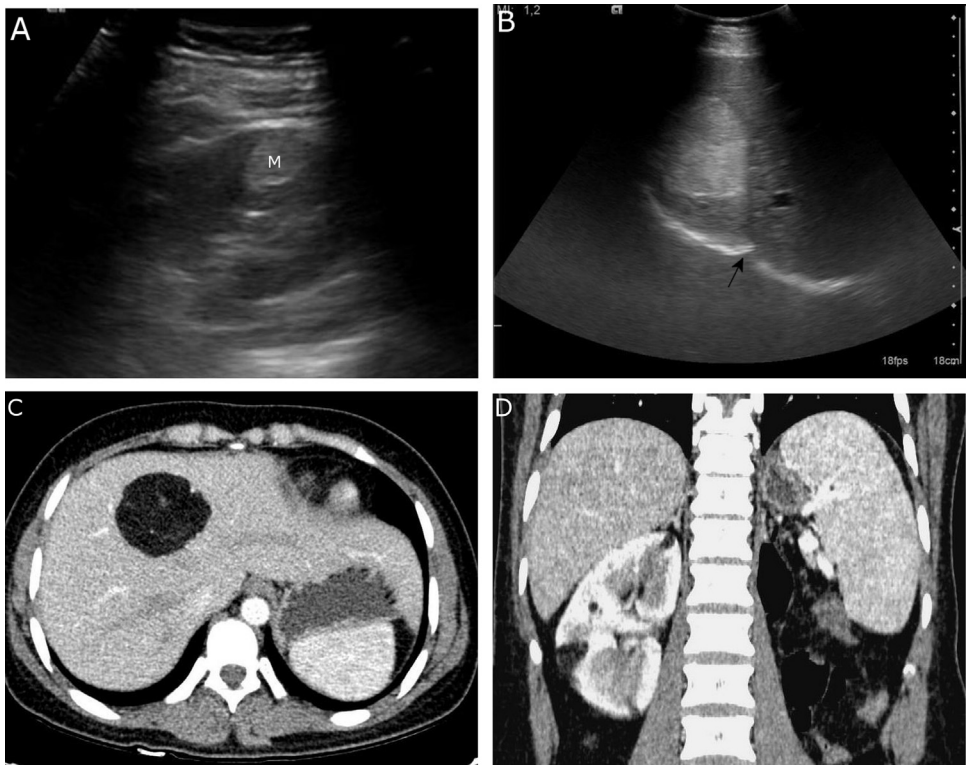

FIG 3. A case of tuberous sclerosis presenting with right renal and liver AMLs. The patient underwent left nephrectomy previously for an AML which bled acutely. (A) Ultrasound of the right kidney showing a hyperechoic mass (*M*) with angular morphology located in the renal cortex. (B) Liver also shows a large hyperechoic lesion in segment IV, causing speed propagation artifact (*arrow*) in the right diaphragm, suggestive of fat content. CECT confirms the diagnosis of hepatic (C) as well as multiple right renal AMLs (D). Note the absence of the left kidney.

However, several other studies have observed early enhancement and subsequent washout in AML, a finding which has been attributed to a larger proportion of angiomatous than myomatous content (Fig 4F and G).[49,59,65]

As AML is hypometabolic, it shows poor uptake on ^{18}F-fluorodeoxyglucose (FDG) PET-CT.[66] Ho et al evaluated dual-tracer PET-CT with ^{18}F-FDG as well as ^{11}C-acetate and observed that AML, low-grade clear cell RCC and chromophobe RCC showed uptake with ^{11}C-acetate but not with ^{18}F-FDG. Papillary RCC and high-grade clear cell RCC showed a reverse pattern.[67]

Four subtypes of lipid-poor AML have been described based on the CT attenuation characteristics and the presence of cysts. Hyperattenuating AMLs are the most common type and are homogenously hyperdense on CT, show T2 hypointensity, diffusion restriction and homogenous postcontrast enhancement. However, no signal drop is apparent on chemical shift imaging. These features are attributed to the presence of dense HMB-45 positive smooth muscles and the absence of fat cells. In contrast, hypoattenuating AML contain cells with microscopic fat, have attenuation in the range of −10 to 45 HU and show signal drop on opposed-phase images. Isoattenuating AMLs are extremely rare and difficult to differentiate from RCC. Some of the hyperattenuating AMLs may contain cystic spaces and are labeled as AML with epithelial cysts.[44]

Differential Diagnoses and the Role of Biopsy

Though the presence of fat of CT in a renal mass offers a reasonably specific diagnosis of AML and helps avoid a biopsy, exceptions are seen. Rarely, RCCs, Wilms tumors, and oncocytomas can contain macroscopic fat, a feature that has been attributed to osseous metaplasia with marrow proliferation or entrapment of perirenal fat by the mass (Fig 5A).[68] Presence of fat due to cholesterol necrosis is seen most commonly with papillary RCC.[69-71] A predominantly exophytic AML may be confused as a well-differentiated perirenal liposarcoma. These liposarcomas, also known as “capsular liposarcomas” due to their close association with the renal capsule, may displace or distort the kidney, however, do not possess the angular morphology of AMLs and are not associated with renal parenchymal defects (Fig 5B and C). The above fact applies to renal sinus liposarcomas as well; however, in cases of primary intrarenal liposarcoma, a parenchymal defect will invariably be present.[72] Presence of large intralesional vessels suggests AML since well-differentiated liposarcomas tend to be relatively avascular. In addition, the vascular pedicle of AML traverses the renal parenchyma, whereas that of liposarcomas often arise from the capsular branches and course around the kidney to supply the tumor. Presence of calcification also strongly favours the diagnosis of liposarcoma.[73] AMLs are also confused with junctional parenchymal defects (JPD), cortical scars and postoperative defects packed with perirenal fat. JPD, which result from incomplete fusion of the renunculi, can be identified by their typical location (junction of upper pole and interpolar region) and communication with the renal sinus fat.

The concept of reserving biopsies only for inoperable RCC, poor surgical candidates, suspected metastases, infection, and lymphoma is outdated. The prospect of undergoing less radical therapeutic options (nephron sparing surgeries or percutaneous ablation) or even conservative therapy has increased the rate of biopsy for renal masses smaller than 3 cm and suspected minimal fat AMLs.[74,75]

Angiomyolipomas with macroscopic fat should be sampled when there is intratumoral calcification and large enhancing component, the target being the enhancing solid component of the tumor. Cytology or core biopsy both can be performed,

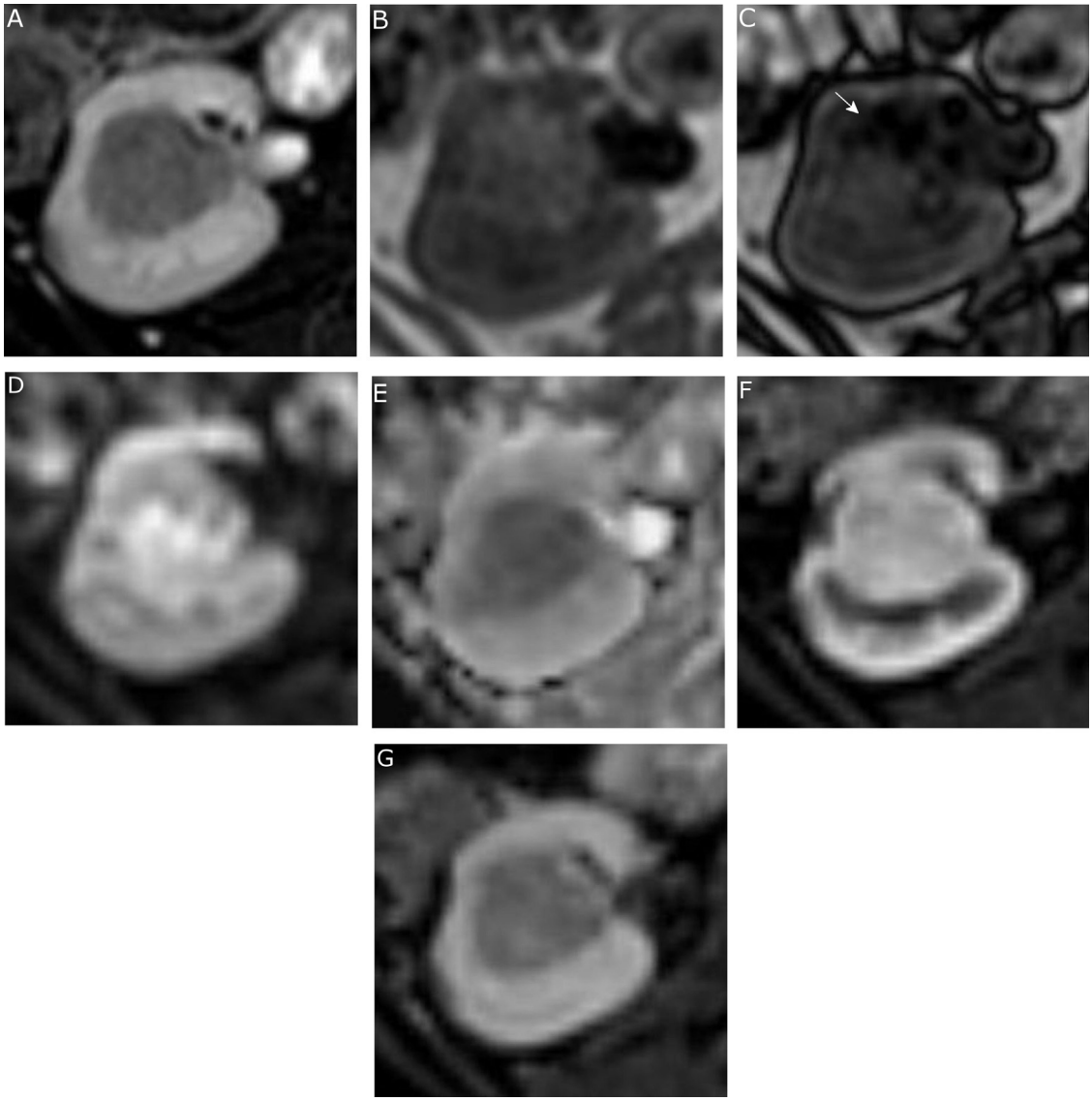

FIG 4. Multiphase MRI of a minimal fat AML showing a well-defined "ball type" mass arising from the kidney in the interpolar location. The mass is homogenously hypointense on T2-weighted images (A). In comparison to the in-phase images (B), there is focal area of signal loss (*arrow*) on the opposed-phase images (C), suggestive of intravoxel microscopic fat. The mass shows diffusion restriction on the trace DWI image (D) as well as the corresponding apparent diffusion coefficient (ADC) map (E). There is early homogenous, intense enhancement in the corticomedullary phase (F), followed by washout in the nephrographic phase (G). This mass is a poor candidate for partial nephrectomy because of its interpolar location and renal sinus involvement.

FIG 5. The imaging differentials for a fat containing renal or perirenal mass. (A) A case of clear cell RCC showing a heterogeneously enhancing mass arising from the lower pole of right kidney, causing invasion of the renal vein and inferior vene cava. Note the area of entrapped renal sinus fat (*arrow*) within the mass. (B) A case of well-differentiated perirenal liposarcoma causing displacement as well as rotation of the right kidney. Note the well-defined interface between the fatty as well as solid components of the tumor and the kidney. A focus of dystrophic calcification is present (*arrow*). A parenchymal defect is distinctly absent and the mass is hypovascular. (C) In comparison, a case of AML shows the parenchymal defect (*D*) in the kidney as well the presence of large intratumoral vessels.

although the latter carries a higher risk of hemorrhage and pseudoaneurysm formation. However, in most cases, the hemorrhage is mild and self limiting with renal biopsy being a safe procedure as long as coagulopathies and bleeding disorders are ruled out.[74] There is no evidence currently suggesting increased incidence of needle track seeding for either of the procedures. In case of TSC, where the diagnosis of minimal fat AML can be made with more confidence, biopsy need to be reserved only for tumors with growth rate more than 0.5 cm per year.[76]

Radiologic Findings of Epitheloid AML

The imaging appearance of EAMLs depends on the proportion of fat. Pure or near-total EAMLs often demonstrate no fat on imaging. The imaging appearances are variable, ranging from hyperattenuating, homogeneously enhancing masses resembling minimal fat AML to heterogeneous enhancing masses with necrosis and hemorrhage like RCC.[77,78] However, calcification is almost never seen. EAML are potentially malignant with risk of extrarenal extension, local recurrence, malignant venous thrombosis (Fig 6), lymphatic and hematogenous metastasis.

Treatment

Asymptomatic AMLs smaller than 4 cm require no treatment, but need to be followed up with annual sonography, CT or MRI. Symptomatic AMLs, regardless of size, can be offered treatment-either partial nephrectomy or SAR. Asymptomatic sporadic AMLs larger than 4 cm carry significant risk of bleed (Fig 7) and traditionally were always offered treatment, however, the new school of thought allows observation in most cases. These authors recommend treatment only when the tumor contains an aneurysm larger than 5 mm, the only finding which reliably predicts future hemorrhage.[79] The 2012 International Tuberous Sclerosis Complex Consensus Group recommends medical management with mTOR inhibitors for all asymptomatic AMLs larger than 3 cm in TSC patients.[76]

Previously, the treatment of choice was surgery and several centers still practice surgery for AML. Hence, it becomes prudent for the radiologist to communicate to the operating surgeon information regarding the imaging features which could predict a potentially difficult surgery. This is best done by the means of any of the several nephrometric scores which help in objectifying decision-making as to the nature of resection (partial vs radical nephrectomy) and the surgical approach (open vs minimal invasive partial nephrectomy) required.[80] These nephrometric scores include the RENAL score, centrality index score and PADUA score. Most experience is with the RENAL score, which assesses the size of the tumor, percentage of exophytic component, nearness to the renal sinus or collecting system, anterior or posterior location and polarity (Table 2).[81] Tumors of low complexity (RENAL score of 4-6 of 12) are more suitable for minimal invasive (laparoscopic) partial nephrectomy. Presence of complex features (diameter above 7 cm, entirely endophytic nature, involvement or renal sinus and interpolar location increase the risk of intraoperative bleeding, operative time, and postoperative complications (renal failure and urinary fistula) and hence necessitate radical nephrectomy. In comparison to RCCs, AML tends to have lower RENAL scores and hence are mostly treated by partial nephrectomy (nephron sparing surgery).

More recently SAR, being minimally invasive, has superceded as the therapeutic option of choice especially in patients with acute bleed and hemodynamic compromise.[6] SAR has been observed to have excellent technical success rate, preserves renal function, is

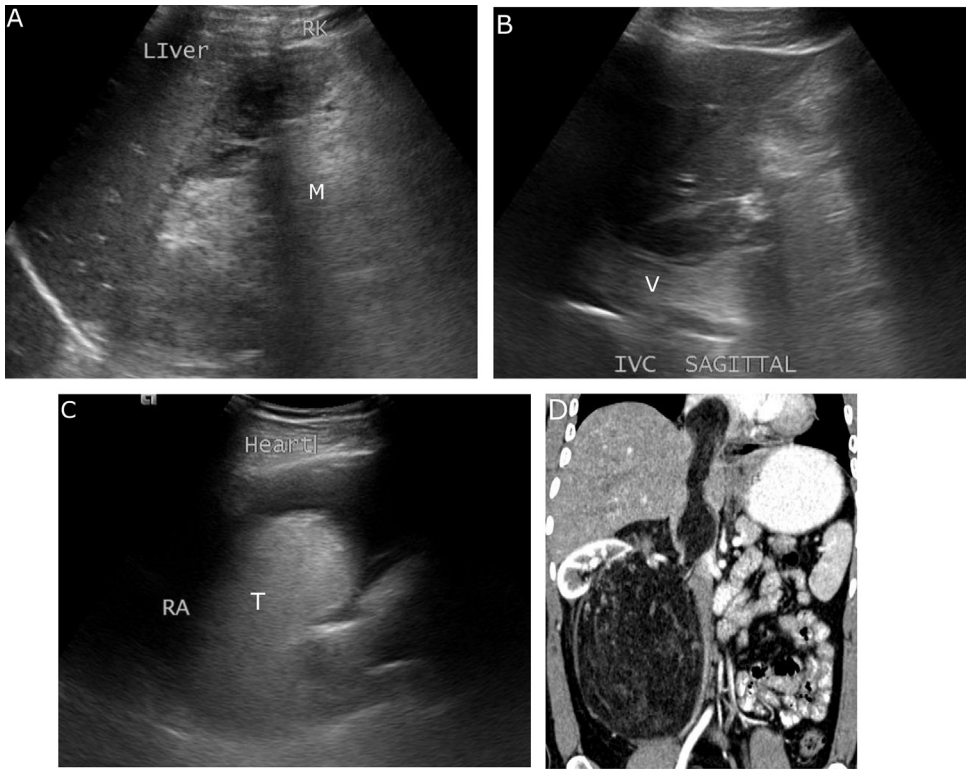

FIG 6. A case of AML causing venous invasion. (A) Ultrasound images, showing a large echogenic mass (M) in the right renal fossa causing anterior displacement of the right kidney (RK). (B) On sagittal images, the inferior vene cava (V) is distended with echogenic thrombus. (C) Four-chamber view of the heart shows extension of the echogenic thrombus (T) into the right atrium (RA). (D) Coronal CECT images confirm the presence of large AML causing anterosuperior displacement of the right kidney with intravascular tumor thrombus extending into the right atrium.

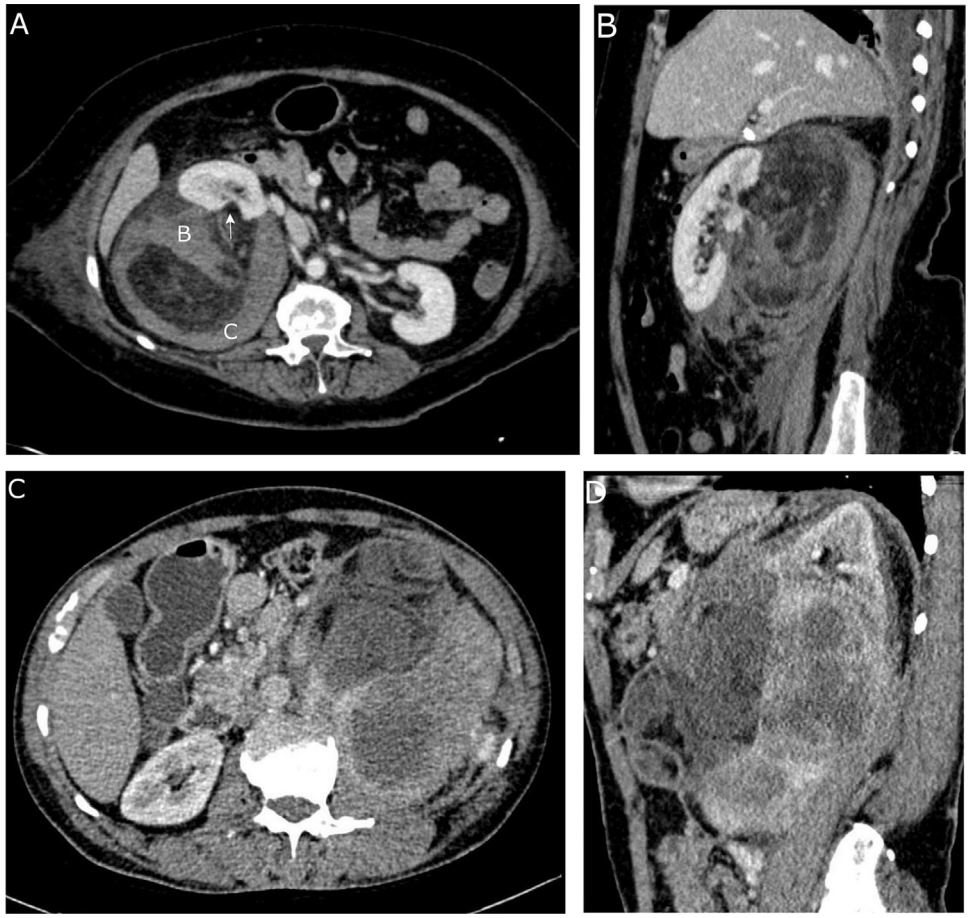

FIG 7. Two cases of renal AML which underwent acute spontaneous hemorrhage. (A and B) The first case shows a large fat containing mass in the right posterior perirenal space with acute intratumoral bleed (B) and layering of clot (C) around the lesion. Note the associated wedge shaped defect (*arrow*) in the posterior renal cortex. (C and D) The second case shows a large left renal mass having intralesional fat and hyperattenuating areas suggestive of acute bleed. The hemorrhage has obscured large areas of fat within the lesion.

suitable for large inoperable tumors, provides rapid stabilization in patients with acute bleed and is associated with lesser post procedural complications than surgery.[82] One systematic review observed a technical success rate of 93% for SAR, with the mean tumor size reduction being 3.4 cm (38%) at follow up after an average of 39 months.[83] Tumor size reduction is better for tumors with larger angiomyomatous component than fat.[84] Repeat embolization was required in 21% of the patients, mostly due to tumor regrowth.[83] Surgery is currently reserved for tumors with diagnostic dilemma, hilar tumors and those with complex vascular anatomy, where the risk of technical failure with SAR is high.

For embolization, superselective catheterization of the feeding artery is done, followed by release of the embolizing agent till stasis of contrast occurs in the vessel (Fig 8). Many embolizing agents have been evaluated including polyvinyl alcohol (PVA), absolute alcohol (with or without iodized oil) and tris-acryl gelatin microspheres (TAGM); however, none has any selective advantage over the others.[85] Absolute alcohol causes protein denaturation, acute thrombosis and permanent occlusion at the arteriolar and capillary level, distal to the collateral supply and hence produces tumor ischemia and necrosis. However, it carries higher risk of reflux and nontarget embolization. Hence, a proximal occlusion balloon often has to be employed to slow the inflow and obtain better control of injection.[86] Microparticles (PVA and TAGM) act by lodging into vessels (arterioles or capillaries, depending on the particle size) and inciting inflammatory reaction, followed by angionecrosis, fibrosis and occlusion. TAGM is preferred since its smooth and spherical shape enables occlusion of the smaller, distal vessels unlike PVA which often tend to aggregate in more proximal vessels due to their irregular shape.[87]

Coils alone should not be used for embolization since they render future re-embolization impossible in cases where tumor reperfusion and growth occurs from recruitment of distal collaterals.[88] In addition, several cases of tumor rebleed have been

TABLE 2
The RENAL nephrometric scoring system

Score	1 point	2 points	3 points
R (maximum diameter in cm)	< 4	> 4 and < 7	> 7
E (exophytic/endophytic)	> 50% exophytic	< 50 exophytic	Completely endophytic
N (nearness to sinus/PCS in mm)	> 7	> 4 and < 7	< 4
A (anterior/posterior location)	No points; *a*, *P*, and *x* descriptors given		
L (location relative to polar lines)	Entirely above or below the polar lines	< 50% of mass between the polar lines	Entire mass or > 50% between the polar lines

Range of possible scores: 4-12. Low complexity (4-6 points), moderate complexity (7-9 points), high complexity (10-12 points); PCS: pelvicalyceal system.

FIG 8. A large left renal AML treated by selective arterial embolization. (A) Coronal CECT images showing a large exophytic mass arising from the lower pole of left kidney having large arterial feeders (*arrows*). (B) Preembolization contrast run of the renal artery showing the large arterial feeders, tumor blush and a small aneurysm (*arrow*). (C) Contrast run after embolization with 20% glue (in lipiodol) showing marked pruning of the feeder arteries and absence of tumor blush. Note the glue cast (*arrows*) in the embolized distal arteries.

observed in the first few days after embolization with microparticles and alcohol. One hypothesis is the increased proximal vascular pressure following occlusion of the distal vascular bed which results in aneurysmal rupture. Hence, one technique could be to perform proximal embolization with coils to reduce the arterial inflow after the distal bed has been occluded with alcohol or microparticles.[89] Of late, glue (N-butyl 2-cyanoacrylate) has been explored since it is cheaper and provides rapid embolization especially in large tumors. A high dilution (1:5) of glue in lipiodol enables rapid distal as well as proximal vascular bed occlusion.[90] In patients with multiple intratumoral aneurysms presenting with acute bleed, it may be difficult to localize the aneurysm responsible for the bleed on angiography since active extravasation is rarely seen. In this context, the presence of mass effect around an aneurysm with displacement of the adjacent vessels (light bulb sign) indirectly indicates perianeurysmal hematoma and the source of bleed.[89]

SAR carries risks of higher rate of recurrence, nontarget embolization and postembolization syndrome. The latter, which had an incidence of 36% in one systematic review, usually occurs in the first 72 hours after embolization due to local and systemic inflammatory response to the ischemic tumor.[83] Symptoms include fever, nausea, flank pain and leucocytosis, and are proportionate to the size of the infarct. It can be managed conservatively with analgesics and anti-inflammatory agents.[91]

Recently, percutaneous or laparoscopic ablation (radiofrequency, microwave, and cryoablation) has also been evaluated in the management of small asymptomatic AMLs.[92,93] However, the experience and evidence with these modalities is insufficient at present. Radiofrequency ablation appears to have excellent technical success rate with favorable complication profile as well as renal function outcomes. It is best suited to solitary tumors smaller than 4 cm and is unsuitable for tumors with large vessels or acute bleed. Transient hematuria and intercostal nerve injury are described complications.[92]

Malignant AML is always managed by partial or radical nephrectomy followed by adjuvant chemotherapy. Pregnancy and poor compliance to follow up are other indications for treatment.[94] The recent discovery of mTOR cascade activation has opened the way for mTOR inhibitors—rapamycin (sirolimus), everolimus, and temsirolimus in the management of AML. These drugs have been used to induce tumor size regression, reduce the gross tumor burden in patients with TSC and as adjuvant therapy in malignant EAML.[95,96]

Conclusion

Classic AML rarely raises diagnostic concerns, however, has to be viewed with caution for the presence of calcification or large enhancing component. When in doubt, sampling is required to avoid missing an RCC. Minimal fat AML can be difficult to differentiate from other renal tumors. It is prudent for the radiologist to look for imaging features which suggest AML. Any renal mass which shows angular morphology, is homogenously hyperattenuating on CT, hypointense on T2-weighted images and shows homogenous hyperenhancement with or without drop of signal on opposed-phase images has to be labeled as “suspicious for minimal fat AML,” so that the patient receives sampling and an unwanted surgery is potentially avoided. In addition, nephrometric scores have to be conveyed to help the surgeon assess the ease of resection when partial nephrectomy is planned. Image-guided interventions have superceded surgery as the treatment of choice and can give excellent outcome with lesser complications when proper technique is used. Newer minimally invasive percutaneous ablation techniques hold promise and may gain more importance in the future once sound scientific evidence becomes available.

References

1. Fittschen A, Wendlik I, Oeztuerk S, et al. Prevalence of sporadic renal angiomyolipoma: A retrospective analysis of 61,389 in- and out-patients. Abdom Imaging 2014;39(5):1009–13.
2. Bauman TM, Potretzke AM, Wright AJ, et al. Partial nephrectomy for presumed renal-cell carcinoma: Incidence, predictors, and perioperative outcomes of benign lesions. J Endourol 2017;31(4):412–7.
3. Rakowski SK, Winterkorn EB, Paul E, et al. Renal manifestations of tuberous sclerosis complex: Incidence, prognosis, and predictive factors. Kidney Int 2006;70(10):1777–82.
4. Budde K, Gaedeke J. Tuberous sclerosis complex-associated angiomyolipomas: Focus on mTOR inhibition. Am J Kidney Dis 2012;59(2):276–83.
5. Yeoh ZW, Navaratnam V, Bhatt R, et al. Natural history of angiomyolipoma in lymphangioleiomyomatosis: Implications for screening and surveillance. Orphanet J Rare Dis 2014;9:151.
6. Seyam RM, Bissada NK, Kattan SA, et al. Changing trends in presentation, diagnosis and management of renal angiomyolipoma: Comparison of sporadic and tuberous sclerosis complex-associated forms. Urology 2008;72(5):1077–82.
7. Neumann HP, Brüggen V, Berger DP, et al. Tuberous sclerosis complex with end-stage renal failure. Nephrol Dial Transplant 1995;10(3):349–53.
8. Bissler J, Cappell K, Charles H, et al. Long-term clinical morbidity in patients with renal angiomyolipoma associated with tuberous sclerosis complex. Urology 2016;95:80–7.
9. Medda M, Picozzi SC, Bozzini G, et al. Wunderlich's syndrome and hemorrhagic shock. J Emerg Trauma Shock 2009;2(3):203–5.
10. Albi G, del Campo L, Tagarro D. Wünderlich's syndrome: Causes, diagnosis and radiological management. Clin Radiol 2002;57(9):840–5.
11. Ünlü C, Lamme B, Nass P, et al. Retroperitoneal haemorrhage caused by a renal angiomyolipoma. Emerg Med J 2006;23(6):464–5.
12. Mathew A, Brahmbhatt B, Rajesh R, et al. Page kidney. Indian J Nephrol 2009;19(4):170–1.
13. Cheng L, Gu J, Eble JN, et al. Molecular genetic evidence for different clonal origin of components of human renal angiomyolipomas. Am J Surg Pathol 2001;25(10):1231–6.
14. Fletcher CDM, Unni KK, Mertens F, Weltgesundheitsorganisation, International Agency for Research on Cancer, editors. Pathology and Genetics of Tumours of Soft Tissue and Bone. [the WHO classification of tumours of soft tissue and bone presented in this book reflects the views of a working group that convened for an editorial and consensus conference in Lyon, France, April

24–28, 2002] (World Health Organization Classification of tumours). Lyon: IARC Press; 2002, 427.
15. Martignoni G, Pea M, Reghellin D, et al. PEComas: The past, the present and the future. Virchows Arch 2008;452(2):119–32.
16. Esheba GES, Esheba NES. Angiomyolipoma of the kidney: Clinicopathological and immunohistochemical study. J Egypt Natl Cancer Inst 2013;25(3):125–34.
17. Köksal IT, Tunç M, Kiliçaslan I, et al. Lymph nodal involvement by renal angiomyolipoma. Int J Urol 2000;7(10):386–9.
18. Garg PK, Jain BK, Kumar A, et al. Fat poor angiomyolipoma with lymphadenopathy: Diagnostic dilemma. Urol Ann 2012;4(2):126–9.
19. Prasad TV, Singh A, Das CJ, et al. An unusually large renal angiomyolipoma peeping into the right atrium. BMJ Case Rep 2016;2016 bcr2016215673.
20. Mittal V, Aulakh BS, Daga G. Benign renal angiomyolipoma with inferior vena cava thrombosis. Urology 2011;77(6):1503–6.
21. Tan YS, Yip KH, Tan PH, et al. A right renal angiomyolipoma with IVC thrombus and pulmonary embolism. Int Urol Nephrol 2010;42(2):305–8.
22. Davis CJ, Barton JH, Sesterhenn IA. Cystic angiomyolipoma of the kidney: A clinicopathologic description of 11 cases. Mod Pathol 2006;19(5):669–74.
23. Aydin H, Magi-galluzzi C, Lane BR, et al. Renal angiomyolipoma: Clinicopathologic study of 194 cases with emphasis on the epithelioid histology and tuberous sclerosis association. Am J Surg Pathol 2009;33(2):289–97.
24. Brimo F, Robinson B, Guo C, et al. Renal Epithelioid Angiomyolipoma with atypia: A series of 40 cases with emphasis on clinicopathologic prognostic indicators of malignancy. Am J Surg Pathol 2010;34(5):715–22.
25. Kawaguchi K, Oda Y, Nakanishi K, et al. Malignant transformation of renal angiomyolipoma: A case report. Am J Surg Pathol 2002;26(4):523–9.
26. Pea M, Bonetti F, Martignoni G, et al. Apparent renal cell carcinomas in tuberous sclerosis are heterogeneous: the identification of malignant epithelioid angiomyolipoma. Am J Surg Pathol 1998;22(2):180–7.
27. Pan C-C, Chung M-Y, Ng K-F, et al. Constant allelic alteration on chromosome 16p (TSC2 gene) in perivascular epithelioid cell tumour (PEComa): Genetic evidence for the relationship of PEComa with angiomyolipoma. J Pathol 2008;214(3):387–93.
28. Thway K, Fisher C. PEComa: Morphology and genetics of a complex tumor family. Ann Diagn Pathol 2015;19(5):359–68.
29. Kenerson H, Folpe AL, Takayama TK, et al. Activation of the mTOR pathway in sporadic angiomyolipomas and other perivascular epithelioid cell neoplasms. Hum Pathol 2007;38(9):1361–71.
30. Martignoni G, Bonetti F, Pea M, et al. Renal disease in adults with TSC2/PKD1 contiguous gene syndrome. Am J Surg Pathol 2002;26(2):198–205.
31. Matsui K, Tatsuguchi A, Valencia J, et al. Extrapulmonary lymphangioleiomyomatosis (LAM): Clinicopathologic features in 22 cases. Hum Pathol 2000;31(10):1242–8.
32. Verma SK, Mitchell DG, Yang R, et al. Exophytic renal masses: Angular interface with renal parenchyma for distinguishing benign from malignant lesions at MR imaging. Radiology 2010;255(2):501–7.
33. Bosniak MA. Angiomyolipoma (hamartoma) of the kidney: A preoperative diagnosis is possible in virtually every case. Urol Radiol 1981;3(3):135–42.
34. Silverman SG, Pearson GD, Seltzer SE, et al. Small (or = 3 cm) hyperechoic renal masses: Comparison of helical and convention CT for diagnosing angiomyolipoma. AJR Am J Roentgenol 1996;167(4):877–81.
35. Simpson E, Patel U. Diagnosis of angiomyolipoma using computed tomography-region of interest or = −10 HU or 4 adjacent pixels or = −10 HU are recommended as the diagnostic thresholds. Clin Radiol 2006;61(5):410–6.
36. Davenport MS, Neville AM, Ellis JH, et al. Diagnosis of renal angiomyolipoma with hounsfield unit thresholds: Effect of size of region of interest and nephrographic phase imaging. Radiology 2011;260(1):158–65.
37. Dyer R, DiSantis DJ, McClennan BL. Simplified imaging approach for evaluation of the solid renal mass in adults. Radiology 2008;247(2):331–43.
38. Takahashi K, Honda M, Okubo RS, et al. CT pixel mapping in the diagnosis of small angiomyolipomas of the kidneys. J Comput Assist Tomogr 1993;17(1):98–101.
39. Kim JY, Kim JK, Kim N, et al. CT histogram analysis: Differentiation of angiomyolipoma without visible fat from renal cell carcinoma at CT imaging. Radiology 2008;246(2):472–9.
40. Simpfendorfer C, Herts BR, Motta-Ramirez GA, et al. Angiomyolipoma with minimal fat on MDCT: Can counts of negative-attenuation pixels aid diagnosis? Am J Roentgenol 2009;192(2):438–43.
41. Chaudhry HS, Davenport MS, Nieman CM, et al. Histogram Analysis of small solid renal masses: Differentiating minimal fat angiomyolipoma from renal cell carcinoma. Am J Roentgenol 2012;198(2):377–83.
42. Catalano OA, Samir AE, Sahani DV, et al. Pixel distribution analysis: Can it be used to distinguish clear cell carcinomas from angiomyolipomas with minimal fat? Radiology 2008;247(3):738–46.
43. Takahashi N, Takeuchi M, Sasaguri K, et al. CT negative attenuation pixel distribution and texture analysis for detection of fat in small angiomyolipoma on unenhanced CT. Abdom Radiol 2016;41(6):1142–51.
44. Jinzaki M, Silverman SG, Akita H, et al. Renal angiomyolipoma: A radiological classification and update on recent developments in diagnosis and management. Abdom Imaging 2014;39(3):588–604.
45. Xie P, Yang Z, Yuan Z. Lipid-poor renal angiomyolipoma: Differentiation from clear cell renal cell carcinoma using wash-in and washout characteristics on contrast-enhanced computed tomography. Oncol Lett 2016;11(3):2327–31.
46. Milner J, McNeil B, Alioto J, et al. Fat poor renal angiomyolipoma: Patient, computerized tomography and histological findings. J Urol 2006;176(3):905–9.
47. Jinzaki M, Tanimoto A, Narimatsu Y, et al. Angiomyolipoma: Imaging findings in lesions with minimal fat. Radiology 1997;205(2):497–502.
48. Colvin SH. Certain capsular and subcapsular mixed tumors of the kidney herein called “capsuloma”1. J Urol 1942;48(6):585–600.
49. Yang C-W, Shen S-H, Chang Y-H, et al. Are there useful CT features to differentiate renal cell carcinoma from lipid-poor renal angiomyolipoma? Am J Roentgenol 2013;201(5):1017–28.
50. Woo S, Cho JY, Kim SH, et al. Angiomyolipoma with minimal fat and non-clear cell renal cell carcinoma: Differentiation on MDCT using classification and regression tree analysis-based algorithm. Acta Radiol Stockh Swed 1987 2014;55(10):1258–69.
51. Karlo CA, Donati OF, Burger IA, et al. MR imaging of renal cortical tumours: Qualitative and quantitative chemical shift imaging parameters. Eur Radiol 2013;23(6):1738–44.
52. Jeong CJ, Park BK, Park JJ, et al. Unenhanced CT and MRI parameters that can be used to reliably predict fat-invisible angiomyolipoma. Am J Roentgenol 2016;206(2):340–7.
53. Jinzaki M, Silverman SG, Tanimoto A, et al. Angiomyolipomas that do not contain fat attenuation at unenhanced CT. Radiology 2005;234(1):311; [author reply 311-312].
54. Silverman SG, Mortele KJ, Tuncali K, et al. Hyperattenuating renal masses: Etiologies, pathogenesis, and imaging evaluation. Radiographics 2007;27(4):1131–43.
55. Takahashi N, Leng S, Kitajima K, et al. Small (4 cm) renal masses: Differentiation of angiomyolipoma without visible fat from renal cell carcinoma using unenhanced and contrast-enhanced CT. Am J Roentgenol 2015;205(6):1194–202.
56. Hodgdon T, McInnes MDF, Schieda N, et al. Can quantitative CT texture analysis be used to differentiate fat-poor renal angiomyolipoma from renal cell carcinoma on unenhanced CT images? Radiology 2015;276(3):787–96.
57. Lee HS, Hong H, Jung DC, et al. Differentiation of fat-poor angiomyolipoma from clear cell renal cell carcinoma in contrast-enhanced MDCT images using quantitative feature classification. Med Phys 2017;44(7):3604–14.
58. Kim JK, Park S-Y, Shon J-H, et al. Angiomyolipoma with minimal fat: Differentiation from renal cell carcinoma at biphasic helical CT. Radiology 2004;230(3):677–84.
59. Sasiwimonphan K, Takahashi N, Leibovich BC, et al. Small (4 cm) renal mass: Differentiation of angiomyolipoma without visible fat from renal cell carcinoma utilizing MR imaging. Radiology 2012;263(1):160–8.
60. Kim JK, Kim SH, Jang YJ, et al. Renal angiomyolipoma with minimal fat: Differentiation from other neoplasms at double-echo chemical shift FLASH MR imaging. Radiology 2006;239(1):174–80.
61. Jhaveri KS, Elmi A, Hosseini-Nik H, et al. Predictive value of chemical-shift MRI in distinguishing clear cell renal cell carcinoma from non–clear cell renal cell carcinoma and minimal-fat angiomyolipoma. Am J Roentgenol 2015;205(1):W79–86.
62. Hindman N, Ngo L, Genega EM, et al. Angiomyolipoma with minimal fat: Can it be differentiated from clear cell renal cell carcinoma by using standard MR techniques? Radiology 2012;265(2):468–77.
63. Sung CK, Kim SH, Woo S, et al. Angiomyolipoma with minimal fat: Differentiation of morphological and enhancement features from renal cell carcinoma at CT imaging. Acta Radiol 2016;57(9):1114–22.
64. Pierorazio PM, Hyams ES, Tsai S, et al. Multiphasic enhancement patterns of small renal masses (≤4 cm) on preoperative computed tomography: Utility for distinguishing subtypes of renal cell carcinoma, angiomyolipoma, and oncocytoma. Urology 2013;81(6):1265–71.
65. Scialpi M, Di Maggio A, Midiri M, et al. Small renal masses: Assessment of lesion characterization and vascularity on dynamic contrast-enhanced MR imaging with fat suppression. AJR Am J Roentgenol 2000;175(3):751–7.
66. Lin C-Y, Chen H-Y, Ding H-J, et al. FDG PET or PET/CT in evaluation of renal angiomyolipoma. Korean J Radiol 2013;14(2):337–42.
67. Ho C-L, Chen S, Ho KMT, et al. Dual-tracer PET/CT in renal angiomyolipoma and subtypes of renal cell carcinoma. Clin Nucl Med 2012;37(11):1075–82.
68. Hélénon O, Merran S, Paraf F, et al. Unusual fat-containing tumors of the kidney: A diagnostic dilemma. Radiographics 1997;17(1):129–44.
69. Couvidat C, Eiss D, Verkarre V, et al. Renal papillary carcinoma: CT and MRI features. Diagn Interv Imaging 2014;95(11):1055–63.
70. Schuster TG, Ferguson MR, Baker DE, et al. Papillary renal cell carcinoma containing fat without calcification mimicking angiomyolipoma on CT. Am J Roentgenol 2004;183(5):1402–4.
71. Prasad SR, Humphrey PA, Catena JR, et al. Common and uncommon histologic subtypes of renal cell carcinoma: Imaging spectrum with pathologic correlation. Radiographics 2006;26(6):1795–806.
72. Israel GM, Bosniak MA, Slywotzky CM, et al. CT differentiation of large exophytic renal angiomyolipomas and perirenal liposarcomas. AJR Am J Roentgenol 2002;179(3):769–73.
73. Ellingson JJ, Coakley FV, Joe BN, et al. Computed tomographic distinction of perirenal liposarcoma from exophytic angiomyolipoma: A feature analysis study. J Comput Assist Tomogr 2008;32(4):548–52.
74. Sahni VA, Silverman SG. Biopsy of renal masses: when and why. Cancer Imaging 2009;9(1):44–55.
75. Silverman SG, Gan YU, Mortele KJ, et al. Renal masses in the adult patient: The role of percutaneous biopsy. Radiology 2006;240(1):6–22.
76. Krueger DA, Northrup H, International Tuberous Sclerosis Complex Consensus Group. Tuberous sclerosis complex surveillance and management:

Recommendations of the 2012 International Tuberous Sclerosis Complex Consensus Conference. Pediatr Neurol 2013;49(4):255–65.
77. Froemming AT, Boland J, Cheville J, et al. Renal epithelioid angiomyolipoma: Imaging characteristics in nine cases with radiologic-pathologic correlation and review of the literature. Am J Roentgenol 2013;200(2):W178–86.
78. Guo B, Song H, Yue J, et al. Malignant renal epithelioid angiomyolipoma: A case report and review of the literature. Oncol Lett 2016;11(1):95–8.
79. Yamakado K, Tanaka N, Nakagawa T, et al. Renal angiomyolipoma: Relationships between tumor size, aneurysm formation, and rupture. Radiology 2002;225(1):78–82.
80. Canter D, Kutikov A, Manley B, et al. Utility of the R.E.N.A.L.—Nephrometry scoring system in objectifying treatment decision-making of the enhancing renal mass. Urology 2011;78(5):1089–94.
81. Parsons RB, Canter D, Kutikov A, et al. RENAL nephrometry scoring system: The radiologist's perspective. AJR Am J Roentgenol 2012;199(3):W355–9.
82. Faddegon S, So A. Treatment of angiomyolipoma at a tertiary care centre: The decision between surgery and angioembolization. Can Urol Assoc J 2011;5(6):E138–41.
83. Murray TE, Doyle F, Lee M. Transarterial embolization of angiomyolipoma: A systematic review. J Urol 2015;194(3):635–9.
84. Planché O, Correas J-M, Mader B, et al. Prophylactic embolization of renal angiomyolipomas: Evaluation of therapeutic response using CT 3D volume calculation and density histograms. J Vasc Interv Radiol 2011;22(10):1388–95.
85. Flum AS, Hamoui N, Said MA, et al. Update on the diagnosis and management of renal angiomyolipoma. J Urol 2016;195(4, Part 1):834–46.
86. Omodon M, Ayuba G, Patel IJ. Review of renal artery embolization for treatment of renal angiomyolipoma. Clin Nephrol Urol Sci 2016;3(1):1.
87. Vaidya S, Tozer KR, Chen J. An overview of embolic agents. Semin Interv Radiol 2008;25(3):204–15.
88. Kothary N, Soulen MC, Clark TWI, et al. Renal angiomyolipoma: Long-term results after arterial embolization. J Vasc Interv Radiol 2005;16(1):45–50.
89. Lenton J, Kessel D, Watkinson AF. Embolization of renal angiomyolipoma: Immediate complications and long-term outcomes. Clin Radiol 2008;63(8):864–70.
90. Bardin F, Chevallier O, Bertaut A, et al. Selective arterial embolization of symptomatic and asymptomatic renal angiomyolipomas: A retrospective study of safety, outcomes and tumor size reduction. Quant Imaging Med Surg 2017;7(1):8–23.
91. Lee S-Y, Hsu H-H, Chen Y-C, et al. Embolization of renal angiomyolipomas: Short-term and long-term outcomes, complications, and tumor shrinkage. Cardiovasc Intervent Radiol 2009;32(6):1171–8.
92. Castle SM, Gorbatiy V, Ekwenna O, et al. Radiofrequency ablation (RFA) therapy for renal angiomyolipoma (AML): An alternative to angio-embolization and nephron-sparing surgery. BJU Int 2012;109(3):384–7.
93. Cristescu M, Abel EJ, Wells S, et al. Percutaneous microwave ablation of renal angiomyolipomas. Cardiovasc Intervent Radiol 2016;39(3):433–40.
94. Nelson CP, Sanda MG. Contemporary diagnosis and management of renal angiomyolipoma. J Urol 2002;168(4 Pt 1):1315–25.
95. Palavra F, Robalo C, Reis F. Recent advances and challenges of mTOR inhibitors use in the treatment of patients with tuberous sclerosis complex. Oxid Med Cell Longev 2017 [cited January 14, 2018]. ⟨https://www.ncbi.nlm.nih.gov/pmc/articles/PMC5366202/⟩.
96. Bissler JJ, McCormack FX, Young LR, et al. Sirolimus for angiomyolipoma in tuberous sclerosis complex or lymphangioleiomyomatosis. N Engl J Med 2008;358(2):140–51.